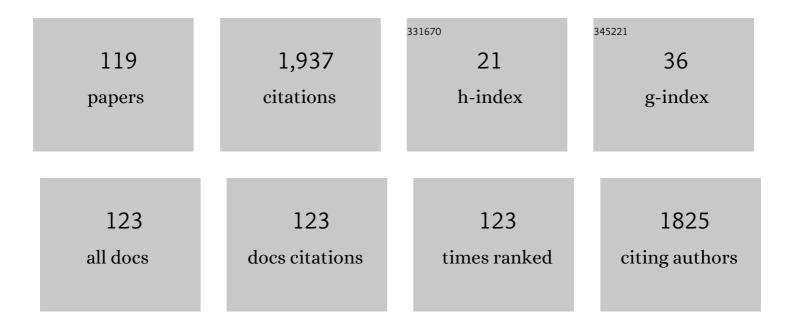
Edouard Asselin

List of Publications by Year in descending order

Source: https://exaly.com/author-pdf/2151517/publications.pdf Version: 2024-02-01



#	Article	IF	CITATIONS
1	Electrochemical and XPS analysis of chalcopyrite (CuFeS2) dissolution in sulfuric acid solution. Electrochimica Acta, 2013, 87, 97-112.	5.2	258
2	Electrochemical evaluation of the surface of chalcopyrite during dissolution in sulfuric acid solution. Electrochimica Acta, 2010, 55, 5041-5056.	5.2	116
3	Electrodeposition and Growth Mechanism of Copper Sulfide Nanowires. Journal of Physical Chemistry C, 2011, 115, 9320-9334.	3.1	76
4	Corrosion of niobium in sulphuric and hydrochloric acid solutions at 75 and 95°C. Corrosion Science, 2007, 49, 694-710.	6.6	69
5	Corrosion of nickel–chromium alloys, stainless steel and niobium at supercritical water oxidation conditions. Corrosion Science, 2010, 52, 118-124.	6.6	52
6	Kinetics of the ferric–ferrous couple on anodically passivated chalcopyrite (CuFeS2) electrodes. Hydrometallurgy, 2012, 125-126, 42-49.	4.3	52
7	The deposition of smooth metallic molybdenum from aqueous electrolytes containing molybdate ions. Electrochemistry Communications, 2012, 15, 78-80.	4.7	50
8	Atmospheric ferric sulfate leaching of chalcopyrite: Thermodynamics, kinetics and electrochemistry. Hydrometallurgy, 2016, 165, 148-158.	4.3	38
9	Electrochemical dissolution of fresh and passivated chalcopyrite electrodes. Effect of pyrite on the reduction of Fe3+ ions and transport processes within the passive film. Electrochimica Acta, 2014, 127, 7-19.	5.2	36
10	Corrosion resistance of hot-dip galvanized steel in simulated soil solution: A factorial design and pit chemistry study. Corrosion Science, 2020, 164, 108310.	6.6	35
11	Influence of Cupric, Ferric, and Chloride on the Corrosion of Titanium in Sulfuric Acid Solutions Up to 85°C. Corrosion, 2014, 70, 29-37.	1.1	30
12	Leaching kinetics of enargite in alkaline sodium sulphide solutions. Hydrometallurgy, 2014, 146, 48-58.	4.3	29
13	Kinetics of Ferric Ion Reduction on Chalcopyrite and its Influence on Leaching up to 150 °C. Electrochimica Acta, 2014, 146, 307-321.	5.2	28
14	Improved corrosion resistance of air plasma sprayed WC-12%Co cermet coating by laser re-melting process. Materials Letters, 2017, 191, 34-37.	2.6	28
15	Scanning electrochemical microscopy screening of CO2 electroreduction activities and product selectivities of catalyst arrays. Communications Chemistry, 2020, 3, .	4.5	28
16	Reducing power consumption in zinc electrowinning. Jom, 2009, 61, 54-58.	1.9	27
17	Leaching of a limonitic laterite in ammoniacal solutions with metallic iron. Hydrometallurgy, 2010, 104, 260-267.	4.3	26
18	Differentiation of the non-faradaic and pseudocapacitive electrochemical response of graphite felt/CuFeS2 composite electrodes. Electrochimica Acta, 2016, 212, 979-991.	5.2	26

#	Article	IF	CITATIONS
19	One-step template-free electrosynthesis of 300μ m long copper sulfide nanowires. Electrochemistry Communications, 2011, 13, 12-15.	4.7	25
20	Laboratory and Pilot Scale Studies of Potassium Extraction from K-feldspar Decomposition with CaCl ₂ and CaCO ₃ . Journal of Chemical Engineering of Japan, 2016, 49, 111-119.	0.6	23
21	Morphology of chalcopyrite leaching in acidic ferric sulfate media. Hydrometallurgy, 2009, 96, 183-188.	4.3	22
22	Effect of Oxygen on the Corrosion Behavior of Alloy 625 from 25â€,toâ€,200°C. Journal of the Electrochemical Society, 2007, 154, C215.	2.9	21
23	Effects of Temperature and Sulfate on the Pitting Corrosion of Titanium in High-Temperature Chloride Solutions. Journal of the Electrochemical Society, 2015, 162, C189-C196.	2.9	21
24	Fluoride induced corrosion of Ti-45Nb in sulfuric acid solutions. Corrosion Science, 2021, 181, 109232.	6.6	21
25	Corrosion of monometallic iron- and nickel-based electrocatalysts for the alkaline oxygen evolution reaction: A review. Journal of Power Sources, 2021, 510, 230387.	7.8	21
26	A new method to improve the corrosion resistance of titanium for hydrometallurgical applications. Applied Surface Science, 2015, 332, 480-487.	6.1	20
27	A review on the electrocatalytic dissociation of water over stainless steel: Hydrogen and oxygen evolution reactions. Renewable and Sustainable Energy Reviews, 2022, 161, 112323.	16.4	20
28	Thermodynamics of the Corrosion of Alloy 625 Supercritical Water Oxidation Reactor Tubing in Ammoniacal Sulfate Solution. Corrosion, 2008, 64, 301-314.	1.1	19
29	Extended validation of an expression to predict ORP and iron chemistry: Application to complex solutions generated during the acidic leaching or bioleaching of printed circuit boards. Hydrometallurgy, 2016, 164, 334-342.	4.3	18
30	Controlling the dissolution of iron through the development of nanostructured Fe-Mg for biomedical applications. Acta Biomaterialia, 2020, 113, 660-676.	8.3	18
31	A Critical Review of the Time-Dependent Performance of Polymeric Pipeline Coatings: Focus on Hydration of Epoxy-Based Coatings. Polymers, 2021, 13, 1517.	4.5	18
32	Determination and Modeling of Vapor–Liquid Equilibria for the Sulfuric Acid + Water + Butyl Acetate + Ethanol System. Industrial & Engineering Chemistry Research, 2013, 52, 3481-3489.	3.7	17
33	Evaluation of the cathodic disbondment resistance of pipeline coatings – A review. Progress in Organic Coatings, 2020, 146, 105728.	3.9	17
34	Characterization of residue generated during medium temperature leaching of chalcopyrite concentrate under CESL conditions. Hydrometallurgy, 2011, 110, 107-114.	4.3	16
35	Copper and Cyanide Extraction with Emulsion Liquid Membrane with LIX 7950 as the Mobile Carrier: Part 1, Emulsion Stability. Metals, 2015, 5, 2034-2047.	2.3	16
36	On the use of a naturally-sourced CuFeS2 mineral concentrate for energy storage. Electrochimica Acta, 2019, 297, 1079-1093.	5.2	16

3

#	Article	IF	CITATIONS
37	<i>In vitro</i> evaluation of antimicrobial efficacy and durability of three copper surfaces used in healthcare. Biointerphases, 2020, 15, 011005.	1.6	16
38	Corrosion evaluation of Ti–6Al–4V manufactured by electron beam melting in Ringer's physiological solution: an in vitro study of the passive film. Journal of Applied Electrochemistry, 2022, 52, 1003-1019.	2.9	16
39	In Situ Electrochemical Analysis of Surface Layers on a Pyrrhotite Electrode in Hydrochloric Acid Solution. Journal of the Electrochemical Society, 2010, 157, C248.	2.9	15
40	The Anodic Passivity of Titanium in Mixed Sulfate-Chloride Solutions. Journal of the Electrochemical Society, 2015, 162, E289-E295.	2.9	15
41	Critical pitting temperature of selective laser melted 316L stainless steel: A mechanistic approach. Corrosion Science, 2021, 185, 109302.	6.6	15
42	The effects of mixtures of acid mist suppression reagents on zinc electrowinning from spent electrolyte solutions. Hydrometallurgy, 2011, 108, 1-10.	4.3	14
43	A Hybrid Mineral Battery: Energy Storage and Dissolution Behavior of CuFeS ₂ in a Fixed Bed Flow Cell. ChemSusChem, 2018, 11, 1533-1548.	6.8	14
44	Electrodeposition of metallic molybdenum and its alloys – a review. Canadian Metallurgical Quarterly, 2019, 58, 1-18.	1.2	14
45	Solubility of AlCl ₃ ·6H ₂ O in the Fe(II) + Mg + Ca + K + Cl + H ₂ O System and Its Salting-Out Crystallization with FeCl ₂ . Industrial & Engineering Chemistry Research, 2013, 52, 14282-14290.	3.7	13
46	Electrochemical detection of corrosion product fouling in high temperature and high pressure solution. Electrochimica Acta, 2013, 100, 101-109.	5.2	12
47	A novel separation process for detoxifying cadmium-containing residues from zinc purification plants. Minerals Engineering, 2014, 64, 1-6.	4.3	12
48	Microstructural, corrosion and mechanical properties of additively manufactured alloys: a review. Critical Reviews in Solid State and Materials Sciences, 2022, 47, 46-98.	12.3	12
49	A Polarization Study of Alloy 625, Nickel, Chromium, and Molybdenum in Ammoniated Sulfate Solutions. Corrosion, 2005, 61, 579-586.	1.1	11
50	Electrochemical properties of metallurgical-grade silicon in hydrochloric acid. Electrochimica Acta, 2009, 54, 6548-6553.	5.2	11
51	Potentiometric titration of hematite and magnetite at elevated temperatures using a ZrO2-based pH probe. Colloids and Surfaces A: Physicochemical and Engineering Aspects, 2014, 444, 144-152.	4.7	11
52	On the refractory nature of precious metal tellurides. Hydrometallurgy, 2017, 169, 488-495.	4.3	11
53	Factors affecting hematite precipitation and characterization of the product from simulated sulphate-chloride solutions at 150â€ ⁻ °C. Hydrometallurgy, 2018, 179, 8-19.	4.3	11
54	Electrochemical Investigation and Identification of Titanium Hydrides Formed in Mixed Chloride Sulfuric Acid Solution. Journal of the Electrochemical Society, 2019, 166, C3096-C3105.	2.9	11

#	Article	IF	CITATIONS
55	Leaching of Mercury from Contaminated Solid Waste: A Mini-Review. Mineral Processing and Extractive Metallurgy Review, 2020, 41, 187-197.	5.0	11
56	Thermo–Kinetic diagrams: The Cu–H2O–Acetate and the Cu-H2O systems. Journal of Electroanalytical Chemistry, 2021, 895, 115467.	3.8	11
57	Electrochemical study of the dissolution of enargite (Cu3AsS4) in contact with activated carbon. Electrochimica Acta, 2013, 107, 525-536.	5.2	10
58	Long-term Hot Corrosion Behavior of Boiler Tube Alloys in Waste-to-Energy Plants. Oxidation of Metals, 2016, 86, 135-149.	2.1	10
59	Corrosion behaviour of X100 pipeline steel under a salty droplet covered by simulated diluted bitumen. Materials Letters, 2018, 222, 196-199.	2.6	10
60	Localised instability of titanium during its erosion-corrosion in simulated acidic hydrometallurgical slurries. Corrosion Science, 2020, 174, 108816.	6.6	10
61	A process for beneficiation of low-grade manganese ore and synchronous preparation of calcium sulfate whiskers during hydrochloric acid regeneration. Hydrometallurgy, 2021, 199, 105533.	4.3	10
62	Microwave pretreatment for enhanced selective nitric acid pressure leaching of limonitic laterite. Journal of Central South University, 2021, 28, 3050-3060.	3.0	10
63	Cobalt loss due to iron precipitation in ammoniacal carbonate solutions. Hydrometallurgy, 2012, 125-126, 144-147.	4.3	9
64	Characterization of anodized titanium for hydrometallurgical applications—Evidence for the reduction of cupric on titanium dioxide. Applied Surface Science, 2013, 283, 705-714.	6.1	9
65	A New Corrosion Mechanism for X100 Pipeline Steel Under Oil-Covered Chloride Droplets. Corrosion, 2018, 74, 947-957.	1.1	9
66	Electrochemical dissolution of chalcopyrite in the presence of thiourea and formamidine disulfide. Hydrometallurgy, 2018, 179, 110-117.	4.3	9
67	Catalytic effect of ethylene thiourea on the leaching of chalcopyrite. Hydrometallurgy, 2020, 196, 105410.	4.3	9
68	General corrosion vulnerability assessment using a Bayesian belief network model incorporating experimental corrosion data for X60 pipe steel. Journal of Pipeline Science and Engineering, 2021, 1, 329-338.	4.8	9
69	Improving Surface Functionality, Hydrophilicity, and Interfacial Adhesion Properties of High-Density Polyethylene with Activated Peroxides. ACS Applied Materials & Interfaces, 2022, 14, 3601-3609.	8.0	9
70	Process Simulation of Sulfuric Acid Recovery by Azeotropic Distillation: Vapor–Liquid Equilibria and Thermodynamic Modeling. Industrial & Engineering Chemistry Research, 2014, 53, 11794-11804.	3.7	8
71	Effect of Fe(III) and Cu(II) on the Passivation of Ti-2 in Acidic Chloride Solutions. Journal of the Electrochemical Society, 2019, 166, C76-C82.	2.9	8
72	An Investigation on the Effects of Organic Additives on Zinc Electrowinning from Industrial Electrolyte. ECS Transactions, 2010, 28, 267-280.	0.5	7

#	Article	IF	CITATIONS
73	Use of EIS to Measure the Rate of H2O2Decomposition on a Bulk Magnetite Electrode in Alkaline Solution. Journal of the Electrochemical Society, 2012, 159, B831-B838.	2.9	7
74	Modeling Phase Equilibria for the Glycine–NH ₄ Cl–Methanol–Water System and Its Application for the Industrial Monochloroacetic Acid Process. Industrial & Engineering Chemistry Research, 2015, 54, 3488-3497.	3.7	7
75	High Temperature Corrosion of Titanium Under Conditions Relevant to Pressure Leaching: Mass Loss and Electrochemistry. Corrosion, 2015, 71, 352-366.	1.1	7
76	Effect of cysteine on the electrochemical dissolution of chalcopyrite. Hydrometallurgy, 2017, 169, 552-563.	4.3	7
77	Effect of retrogression and reâ€aging (RRA) heat treatment on the corrosion behavior of B206 aluminum–copper casting alloy. Materials and Corrosion - Werkstoffe Und Korrosion, 2018, 69, 998-1015.	1.5	7
78	Kinetics of Passive Film Growth on 304 Stainless Steel in H2SO4 Pickling Solution under Chemical Oxidation. Corrosion, 2018, 74, 705-714.	1.1	7
79	Electrosynthesis of metallic molybdenum from water deficient solution containing molybdate ions and high concentrations of acetate. Surface and Coatings Technology, 2019, 357, 567-574.	4.8	7
80	Water transport through epoxy-based powder pipeline coatings. Progress in Organic Coatings, 2022, 168, 106874.	3.9	7
81	Kinetic study of the dissolution of metallic nickel in sulphuric acid solutions in the presence of different oxidants. Canadian Journal of Chemical Engineering, 2016, 94, 1872-1879.	1.7	6
82	Dissolution Kinetics of Pure Zinc: The Effect of Bulk Solution Concentration and Temperature Studied by the Lead-In Pencil Electrode Technique. Journal of the Electrochemical Society, 2017, 164, C758-C767.	2.9	6
83	Charge Transport Characteristics of the Passive Oxide Film Formed on 3D Printed 316 L Stainless Steel in the Presence of Fe ^{II} /Fe ^{III} Species. Journal of Physical Chemistry C, 2020, 124, 21435-21445.	3.1	6
84	Three phase corrosion of pipeline steel: Size effects of deposited solids under water droplets and an oil diffusion barrier. Journal of Pipeline Science and Engineering, 2021, 1, 137-147.	4.8	6
85	Antimicrobial efficacy and durability of copper formulations over one year of hospital use. Infection Control and Hospital Epidemiology, 2022, 43, 79-87.	1.8	6
86	Electron beam surface remelting enhanced corrosion resistance of additively manufactured Ti-6Al-4V as a potential in-situ re-finishing technique. Scientific Reports, 2022, 12, .	3.3	6
87	Vapor–Liquid Equilibria for the ZnSO4–H2SO4–H2O and MgSO4–H2SO4–H2O Systems at (30, 60, 90),) _T j ETQq	1 ₅ 1 0.784 <mark>3</mark> 1
88	Solubility Measurement and Chemical Modeling of MgSO ₄ ·7H ₂ O in the Ti(SO ₄) ₂ –H ₂ SO ₄ –H ₂ O System. Journal of Chemical & Engineering Data, 2016, 61, 2363-2370.	1.9	5
89	The dissolution kinetics and salt film precipitation of Zn and Fe in chloride solutions: Importance of the common-ion effect and diffusivity. Corrosion Science, 2019, 146, 152-162.	6.6	5
90	The Mineral Battery: Combining Metal Extraction and Energy Storage. Joule, 2020, 4, 4-9.	24.0	5

#	Article	IF	CITATIONS
91	Chemical oxidation of <scp>highâ€density</scp> polyethylene: Surface energy, functionality, and adhesion to liquid epoxy. Journal of Applied Polymer Science, 2021, 138, 50999.	2.6	5
92	On the Development of Thermo-Kinetic Eh-pH Diagrams. Metallurgical and Materials Transactions B: Process Metallurgy and Materials Processing Science, 2012, 43, 1277-1283.	2.1	4
93	The Effect of Chloride Ions on the Passive Films of Titanium in Sulfuric Acids. Solid State Phenomena, 0, 227, 67-70.	0.3	4
94	Etching Induced Stepped Nanostructure on Pb(Mg _(1–<i>x</i>/2) Mn _(<i>x</i>/2) W _{1/2})O ₃ Ceramics. Journal of the American Ceramic Society, 2016, 99, 1125-1128.	3.8	4
95	Amorphous iron phases in medium temperature leach residues and associated metal loss. International Journal of Mineral Processing, 2016, 148, 65-71.	2.6	4
96	Dependence of the Electrochemical and Passive Behavior of the Lead-Acid Battery Positive Grid on Electrode Surface Roughness. Corrosion, 2017, 73, 1359-1366.	1.1	4
97	Failure investigation of stainless steel anodes used in gold electrowinning. Engineering Failure Analysis, 2019, 106, 104183.	4.0	4
98	Integration of Cu extraction and Zn electrowinning processes for energy storage. Journal of Cleaner Production, 2020, 253, 119779.	9.3	4
99	CaCO ₃ Precipitation Kinetics in the System CaCl ₂ –CO ₂ –Mg(OH) ₂ –H ₂ O for Comprehensive Utilization of Soda Production Wastes. ACS Sustainable Chemistry and Engineering, 2021, 9, 398-410.	6.7	4
100	Fe(III) Precipitation and Copper Loss from Sulphate-Chloride Solutions at 150 °C: A Statistical Approach. Metals, 2020, 10, 669.	2.3	3
101	A New Process for Peracetic Acid Production from Acetic Acid and Hydrogen Peroxide Based on Kinetic Modeling and Distillation Simulation. Industrial & Engineering Chemistry Research, 2022, 61, 339-348.	3.7	3
102	Estimation of Thermodynamic Properties of Aqueous Iron and Cobalt Ammines at Elevated Temperatures. Metallurgical and Materials Transactions B: Process Metallurgy and Materials Processing Science, 2010, 41, 520-526.	2.1	2
103	Electrochemical and corrosion behaviour of stainless steels 316L and 317L in chloridised ammonium sulphate solution. Canadian Metallurgical Quarterly, 2012, 51, 471-484.	1.2	2
104	Novel reagents for iron and sulphur control in medium temperature leaching of sulphide concentrates. Canadian Metallurgical Quarterly, 2017, 56, 382-392.	1.2	2
105	Aqueous Corrosion of Deformed Steel Under Simulated Diluted Bitumen. Corrosion, 2019, 75, 1194-1206.	1.1	2
106	The Effects of Chloride Droplet Properties on the Underoil Corrosion of API X100 Pipeline Steel. Corrosion, 2019, 75, 1051-1064.	1.1	2
107	Corrosion of cast iron pipelines buried in Fraser River silt subject to climate-induced moisture variations. Acta Geotechnica, 2021, 16, 873-884.	5.7	2
108	Communication—The Galvanic Effect on the Under-Deposit Corrosion of Titanium in Chloride Solutions. Journal of the Electrochemical Society, 0, , .	2.9	2

#	Article	IF	CITATIONS
109	Ex Situ Examination of Matrix and Inclusions of API-X100 before and after Exposure to Bitumen at Elevated Temperature. Materials, 2021, 14, 5007.	2.9	2
110	Preparation of strontium carbonate via celestite leaching in NaHCO3 using two interconnected reactors. Hydrometallurgy, 2021, 204, 105729.	4.3	2
111	Evaluating the antimicrobial activity of copper surfaces against Pseudomonas aeruginosa and Staphylococcus aureus 1 year after use in a microbiology laboratory. Journal of Hospital Infection, 2022, 123, 186-188.	2.9	2
112	Solubility and Modeling of Li ₂ SO ₄ ·H ₂ O in Aqueous H ₂ SO ₄ –MgSO ₄ Solutions for Lithium Extraction from Spodumene. Journal of Chemical & Engineering Data, 2022, 67, 919-931.	1.9	2
113	Turning Bulk Titanium into Rutile Nanorods in One Step: Synthesis, Mechanism, and Application. Crystal Growth and Design, 2016, 16, 1583-1590.	3.0	1
114	FIB/SEM Study of Pitting and Intergranular Corrosion in an Al-Cu Alloy. Corrosion, 2017, 73, 927-941.	1.1	1
115	Electrodeposition of Aluminum onto Copper-Coated Printed Circuit Boards. Journal of the Electrochemical Society, 2017, 164, D729-D736.	2.9	1
116	Predicting the External Corrosion Rate of X60 Pipeline Steel: A Mathematical Model. Metals, 2021, 11, 583.	2.3	1
117	Particle concentration distribution measurements in stirred tanks using a new experimental technique: time and frequency domain analyses. Canadian Metallurgical Quarterly, 2015, 54, 289-296.	1.2	0
118	Method of developing Thermo–Kinetic diagrams: The Cu–H2O–acetate and the Cu-H2O systems. MethodsX, 2021, 8, 101539.	1.6	0
119	Passivity Breakdown of Copper in Borate Buffer Solutions Containing Clâ'', SO42â'', and NO3â''. Corrosion, 2022, 78, 865-875.	1.1	0